

# Design and Implementation of an Optimized Sliding Mode Controller and Compared with a Conventional MPPT Controller for a Solar System

VENKATA RATNAM KOLLURU<sup>\*</sup>, SHIVA SHANKAR SARODE<sup>#</sup>, RAJESH KUMAR PATJOSHI<sup>\*</sup>, KAMALAKANTA MAHAPATRA<sup>\*</sup>, BIDYADHAR SUBUDHI<sup>#</sup>

<sup>\*</sup>Department of ECE, <sup>#</sup>Department of EEE

National Institute of Technology

Rourkela, Odisha

INDIA

kvrnitrkl@gmail.com

*Abstract:* - This article gives a broad idea about Sliding Mode Controller (SMC) implementation to a DC-DC Boost Converter for a Photovoltaic (PV) system to track Maximum Power Point (MPP). SMC implementation meets three conditions like (i) Hitting, (ii) Existence and (iii) Stability. Single exponential PV model is designed for lighting applications, and PV output is connected to a Boost converter to regulate and increase the voltage up to desired level. SMC is implemented in a feedback manner with capacitor voltage and inductor current. The steady state condition occurred at around 0.1sec, and tracking 1.13% extra power at Standard Test Conditions (STC). The results of SMC are compared with Incremental conductance (Inc Cond) Maximum Power Point Tracking (MPPT) controller; the models are simulated in MATLAB/SIMULINK.

*Key-Words:* - DC DC Boost Converter, Incremental Conductance Controller, Maximum Power Point, Photovoltaic, SMC, STC

## 1 Introduction

Solar power has extraordinary potential as a renewable energy generation source due to the plenty of solar power and the resulting pollution free generation of direct current. A PV system generates DC electricity when sun rays fall on a PV array. The PV power generation is based on the principle of the photovoltaic effect [1], [2]. With the advent of silicon p-n junctions, the photoelectric current is able to produce power due to inherent voltage drop across the junction [3]. However, such power generation is well-known for the nonlinear relationship between the current and voltage of the photovoltaic cell. There is a unique point at which the photovoltaic cell produces maximum power; at this point, the rate of change of power with respect to the voltage is equal to zero. There are several power management issues concerning improvement in the conversion efficiency of a PV array, thus maximizing PV power output. PV array has to be operated at MPP in order to extract maximum power output. The maximum power of the PV array changes with shading and/or climatic conditions [3]. The PV output current/voltage changes with solar irradiation levels, whereas the PV output voltage changes with temperature of the PV array. Thus, an important challenge in a PV system is to ensure that

maximum energy [3] is generated from the PV array with a dynamic variation of its output characteristic when connected to a variable load.

A remedy for this problem is placing a power converter between the PV array and load, which could dynamically change the impedance of the circuit by using a control algorithm [4]. DC DC Converters are required to regulate the output voltage at a required level [3], [4]. In this paper, DC DC Boost (step up) converter is used, that has a capability of providing an output voltage which is higher than the input voltage.

The novel SMC approach is acknowledged as one of the advantageous and robust controller for non linear plants operating under varying conditions [5] - [14]. Here, in order to approach the SMC, mathematical modeling of SMC should meet the conditions like hitting, existence and stability, which are part of sliding mode control theory [5]. SMC is to employ a certain sliding surface as a reference path such that the trajectory of the controlled system is directed to the desired equilibrium point [6], [11]. The frequency oscillations may occur in the control process which is reflected in the actual behavior of the trajectory, called as chattering [12]. The trajectory 'S' chatters along the surface and move towards the origin.

The conventional Inc Cond MPPT controller with fixed step size developed by using MATLAB/SIMULINK. This technique is one of the best techniques to track Maximum Power Point [15]-[18]. This MPPT control technique is measuring the incremental changes in PV array current and voltage to predict the effect of voltage change. Inc Cond controller maintains the MPP voltage until the irradiation changes and the process is repeated[19], [20]. MPP is located at the knee of the I-V curve [16].

Section II of this article presents a mathematical modeling of a PV cell explanation and results. Section III is devoted for a DC DC boost converter with state space analysis and results. Section IV is dedicated to design and implementation of modified SMC for a boost converter. Section V shows the implementation of an Inc Cond MPPT controller. Section VI summarizes the comparison and discussion on simulation results (SMC with Inc Cond) and finally conclusions end the paper in Section VII.

**2 PV Device Modeling**

PV is one of the methods of renewable energy generations, which means generating electrical power by converting solar irradiation into direct current. Now, PV is one of the popular renewable energy generation sources due to the accessibility of solar energy and resulting emanation of free generation [8]. The basic diagram of a PV cell is shown in Fig. 1. When the sun light falls on solar panel, it converts into direct current. The current source is connected in parallel to a diode, the current through the diode D is  $I_d$  and the diode is connected in a reverse direction to regulate the voltage of a PV cell.

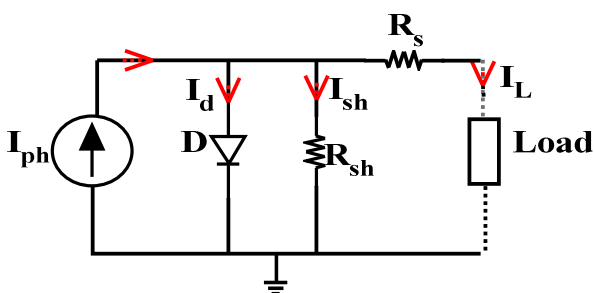


Fig. 1. Circuit of a PV cell single diode model

Two resistors are connected (in series and in parallel) to the current source. Generally  $R_{sh}$  (parallelly connected resistor) is very high and  $R_s$  (series connected resistor) is almost equal to zero, so, the maximum current will flow to the output side. A series resistor  $R_s$ , which determines the

downward slope of I-V curve in PV cell near  $V_{oc}$ , represents the internal resistance of the cell. A shunt resistor  $R_{sh}$ , which determines the slope of the line at a top of I-V curve nearer to  $I_{sc}$  [8], controls the leakage current from cell to ground, and is usually small enough to be neglected. The diode current equation expressed [1] is as follows:

$$I_d = I_0[e^{qV_d/nkT} - 1] \tag{1}$$

Where,  $q$  = charge of the electron,  $V_d$  = Diode voltage,  $k$  = Boltzman’s constant,  $T$ =Absolute temperature,  $n$ =Ideality factor,  $I_0$ =Saturation current.

$$I_{ph} - I_d = I_L \tag{2}$$

Substitute (1) in (2)

$$I_{ph} - I_0[e^{qV_d/nkT} - 1] = I_L \tag{3}$$

After solving (3), which can be expressed in terms of voltage is in the following equation

$$V_L = \frac{nkT}{q} \ln\left(\frac{I_{ph} - I_L}{I_0} + 1\right) - I_L R_s \tag{4}$$

the final expression of PV cell is:

$$V_L = \frac{nkT}{q} \left[ \ln\left(\frac{I_{ph} - I_L}{I_0} + 1\right) - \frac{V_L + I_L R_s}{R_{sh}} \right] - I_L R_s \tag{5}$$

After mathematical modeling of a PV cell is done, we simulated it in MATLAB/SIMULINK and obtained PV characteristic curves. The waveforms are shown in Fig. 2 are calculated at STC.

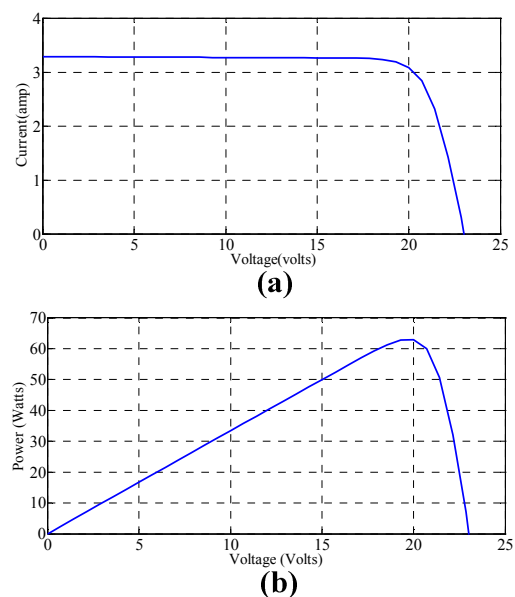


Fig. 2 (a) -V and (b)P-V characteristic curve at STC

PV cells are connected in series mode for addition of voltages and connected in parallel for current summation. The simulated PV model extracted 23V voltage and 3.4A current. If any temperature or irradiation change occurs in weather, then changes in characteristic curves occurred. Fig. 3 shows PV characteristic curves maintaining same temperature and varied irradianations. Here the temperature kept at 25°C and irradiation levels are changing from 1000, 800, 600 and 400 respectively.

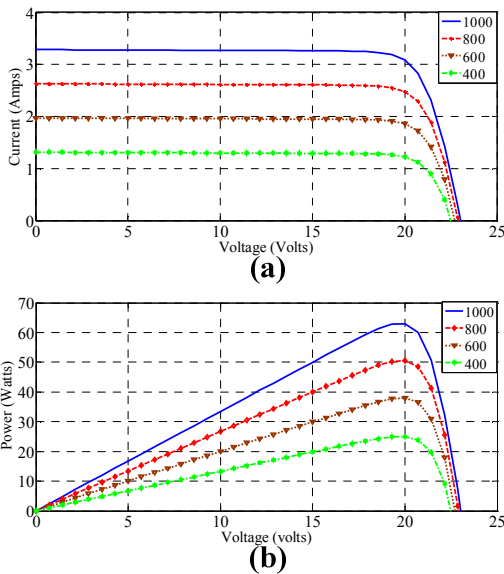


Fig. 3 (a)I-V and (b)P-V characteristic curves at different temperature

### 3 Controller Based Boost Converter

The DC DC boost converter is also called as a step up converter; it has a capability of providing the output voltage higher than the input voltage [6], [8], [12]. The circuit diagram of the conventional controller based boost converter [3] is shown in Fig. 4. The boost converter functioning will depends on the switch “ON and OFF”. The diode ‘D’ blocks the reverse flow of current when the switch is turned ON. The equivalent circuit diagram of the boost converter when the transistor is ‘ON’ is shown in Fig. 5.

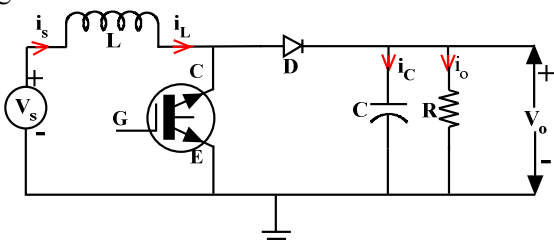


Fig. 4. Conventional Boost Circuit

When the transistor is turned ON, the current

flows from the supply to the inductor L, and at this condition the diode ‘D’ is reverse biased and it does not conduct. Hence the inductor stores the current, then inductor current rises, and the capacitor ‘C’ maintains the voltage ‘V<sub>o</sub>’

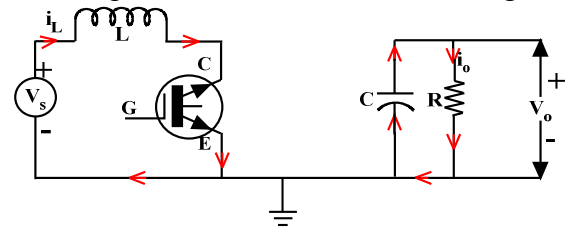


Fig. 5. Equivalent circuit when the transistor is ON

and supplies current ‘i<sub>o</sub>’. The mathematical model of a boost converter when the transistor is ON can be expressed in state space [5] as follows:

$$\begin{bmatrix} \frac{dI_L}{dt} \\ \frac{dV_o}{dt} \end{bmatrix} = \begin{bmatrix} 0 & 0 \\ 0 & -\frac{1}{CR} \end{bmatrix} \begin{bmatrix} I_L \\ V_o \end{bmatrix} + \begin{bmatrix} \frac{1}{L} \\ 0 \end{bmatrix} V_s \tag{6}$$

$$V_o = \begin{bmatrix} 0 & -\frac{1}{CR} \end{bmatrix} \begin{bmatrix} I_L \\ V_o \end{bmatrix} \tag{7}$$

When the switch is turned OFF, the inductor generates a large voltage to maintain the current i<sub>L</sub> in the same direction and now the diode D is forward biased and it starts conducting. The equivalent circuit diagram of boost converter when transistor gets OFF, is shown in Fig. 6.

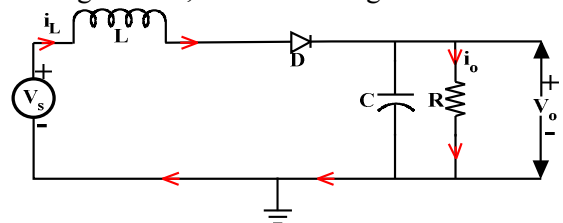


Fig. 6. Equivalent circuit when the transistor is OFF

Hence the output voltage can be expressed as

$$V_o = V_s + L \frac{di_L}{dt} \tag{8}$$

Thus the output voltage of the converter is higher than the supply voltage V<sub>s</sub>, also called as step-up operation. The voltage induced in the inductor adds to the supply voltage and this total voltage appears as output voltage; at that situation the capacitor C also charges to the boosted voltage. The inductor and supply voltage provides energy to the load when the transistor is turned OFF. Current through the inductor decreases because its stored energy goes on reducing. After some time the transistor is again turned ON and the cycle repeats. The mathematical model of a boost converter when the transistor is OFF can be expressed in [3], [8] state space as

$$\begin{bmatrix} \frac{dI_L}{dt} \\ \frac{dV_o}{dt} \end{bmatrix} = \begin{bmatrix} 0 & -\frac{1}{L} \\ \frac{1}{C} & -\frac{1}{CR} \end{bmatrix} \begin{bmatrix} I_L \\ V_o \end{bmatrix} + \begin{bmatrix} I_L \\ 0 \end{bmatrix} [V_s] \quad (9)$$

$$V_o = \begin{bmatrix} \frac{1}{C} & -\frac{1}{CR} \end{bmatrix} \begin{bmatrix} I_L \\ V_o \end{bmatrix} \quad (10)$$

The following results have taken from converter circuit, shown in Fig. 6. These results are exactly matched to the working principle of the boost converter.

### 4 Modified Sliding Mode Controller

The MPPT with SMC for boost converter is a method which improves the deteriorations that originates an additional integral control variable into the constant frequency SMC [5]. The involvement of SMC is to enhance the robustness and regulation of the system [8]. Therefore, the aforementioned uses, mulling over the control performance and simplicity of implementation, adopting an SMC is a better option. SMC introduces a linear combination of system states, which has the same order of the converter [5]-[7].

The fundamental principle of an SMC is to design a particular sliding manifold in its control law that will preside over the trajectory of the state variables towards the required operating point. In case of a boost converter as it has a single switch, it is apt to adopt a control law for a switching function [6] as

$$u = \frac{1}{2}(1 + \text{sgn}(S)) \quad (11)$$

In this case, 'S' is illustrated as

$$S = \alpha_1 x_1 + \alpha_2 x_2 + \alpha_3 x_3 = J^T x \quad (12)$$

with  $J^T = [\alpha_1 \ \alpha_2 \ \alpha_3]$  and  $\alpha_1, \alpha_2, \alpha_3$  representing the control parameters also considered as sliding coefficients,  $x_1, x_2, x_3$  are the state feedback variables which are to be controlled. By equating  $S=0$ , a sliding plane can be acquired. The aim of the designer is to determine the state of switching function 'u' and also to choose appropriate values of  $\alpha_1, \alpha_2$  and  $\alpha_3$  such that the controller satisfies the hitting, SM existence and stability conditions [6].

#### 4.1 Hitting

The design of SMC to meet the hitting condition is straightforward in the case of power converters. Now the state variables can be expressed in the form of

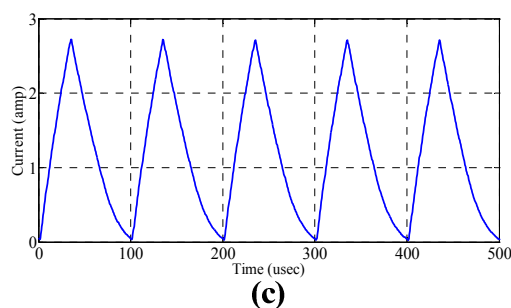
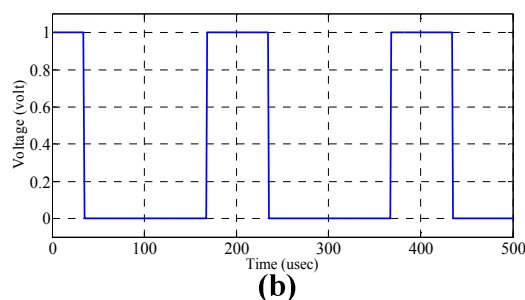
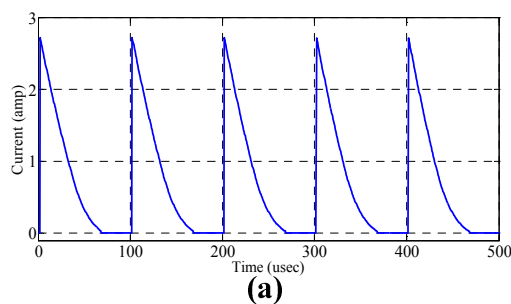


Fig. 7. Results of Boost converter (a) Diode current, (b) Gate voltage, (c) Inductor current.

$$\begin{bmatrix} x_1 \\ x_2 \\ x_3 \end{bmatrix} = \begin{bmatrix} V_{ref} - \beta V_o \\ \frac{d(V_{ref} - \beta V_o)}{dt} \\ \int (V_{ref} - \beta V_o) dt \end{bmatrix} \quad (13)$$

In order to design the hitting condition, it is sufficient to depend only on the immediate state variable  $x_1$ , which is predominant during the reaching phase of 'S'. The resulting control function in this configuration is

$$u = \begin{cases} 1 = ON, & \text{When } S > 0 \\ 0 = OFF, & \text{When } S < 0 \end{cases} \quad (14)$$

Thus, the method ensures fulfillment of hitting condition of the SMC, which is nearly related to the way in which the hysteresis controller switching states are designed.

#### 4.2 SM Existence

With the switching states of the converter determined, the next step is to select the sliding coefficients that fulfills the condition for SM existe

coefficients  $\alpha_1, \alpha_2$  and  $\alpha_3$  that fulfills the condition for SM existence. Now, by inspecting a local reachability condition of the state trajectory, i.e.,

$$\lim_{s \rightarrow 0} S \cdot \dot{S} < 0 \quad (15)$$

$$\dot{S} = J^T \dot{x} \quad (16)$$

$$\dot{x} = Ax + Bu + D \quad (17)$$

Case 1:  $S \rightarrow 0^+, \dot{S} < 0$

Substitution of  $v_{s \rightarrow 0^+} = \bar{u} = 0$  gives

$$-\alpha_1 \frac{\beta i_c}{C} + \alpha_2 \frac{\beta i_c}{r_L C^2} + \alpha_3 (V_{ref} - \beta V_o) < 0 \quad (19)$$

Case 2:  $S \rightarrow 0^-, \dot{S} > 0$

Substitution of  $v_{s \rightarrow 0^-} = \bar{u} = 1$  gives

$$-\alpha_1 \frac{\beta i_c}{C} + \alpha_2 \frac{\beta i_c}{r_L C^2} + \alpha_3 (V_{ref} - \beta V_o) - \alpha_2 \frac{\beta V_i}{LC} + \alpha_2 \frac{\beta V_o}{LC} > 0 \quad (20)$$

Finally, the combination of the above two equations gives the simplified existence condition as follows

$$0 < \beta L \left( \frac{\alpha_1}{\alpha_2} - \frac{1}{r_L C} \right) i_c - LC \frac{\alpha_3}{\alpha_2} (V_{ref} - \beta V_o) < \beta (V_o - V_i) \quad (21)$$

The group of sliding coefficients ( $\alpha_1, \alpha_2$  and  $\alpha_3$ ) for the controller of the boost converter must obey to its stated inequalities. It is important that the circuit tolerances and operating range of conditions are taken into consideration when evaluating the stated inequalities. This confirms the fulfillment of the SM existence condition for the full operating range of the converters.

### 4.3 Stability

The selected sliding coefficients ( $\alpha_1, \alpha_2$  and  $\alpha_3$ ) should satisfy the stability condition simultaneously, apart from the fulfillment of SM existence condition. The relation between the sliding coefficients to the dynamic response of the converter during SM operation is

$$\alpha_1 x_1 + \alpha_2 \frac{dx_1}{dt} + \alpha_3 \int x_1 dt = 0 \quad (22)$$

The above equation can be rearranged into standard second order system from in which the design of the sliding coefficients ( $\alpha_1, \alpha_2$  and  $\alpha_3$ ) will give one of the three possible types of responses like under damped, critical damped and over damped. Therefore, selection of sliding coefficients can be easily done by converter response time and voltage peak over shoot specifications.

For an SM voltage controller the switching logical function ‘u’ is obtained by the combination of control parameters[5]  $x_1, x_2$  and  $x_3$  by utilizing the computation of state trajectories.

$$S = \alpha_1 x_1 + \alpha_2 x_2 + \alpha_3 x_3 = J^T x \quad (23)$$

where  $\alpha_1, \alpha_2$  and  $\alpha_3$  are considered as control parameters.

By imposing  $S=0$ , a sliding line is obtained. The main aim of using sliding line is to serve as a periphery to split the phase trajectory, which reaches and tracks the sliding line affirming a system is stable. From Fig. 8, it can be observed that the phase trajectory is at any arbitrary position below the sliding line ( $S=0$ ) e.g., point ‘P’,  $u=1$  is employed such that the trajectory is directed towards the sliding line. Similarly, when the trajectories above the sliding line e.g., point ‘Q’,  $u=0$  is employed for the trajectory to be directed towards the sliding line.

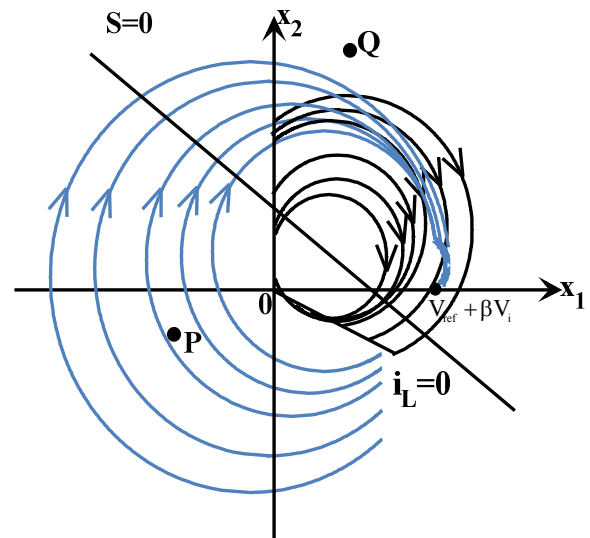
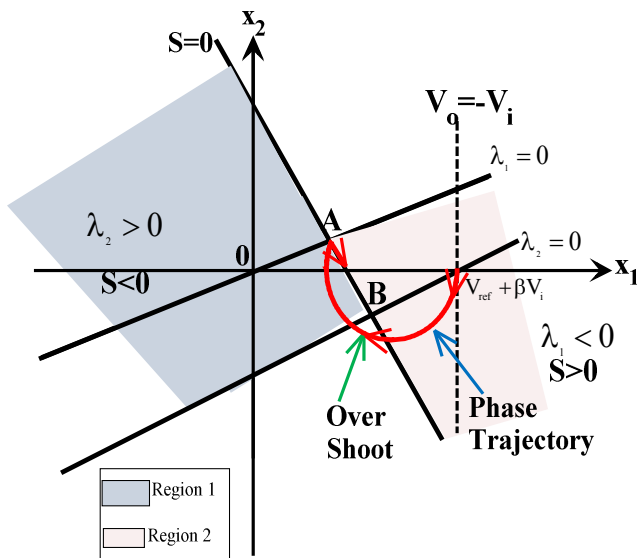


Fig. 8. Plot of phase trajectories of the substructures corresponding  $u=1$  and  $u=0$  for different starting positions of  $x_1$  and  $x_2$ .

$$\lambda_1 = (LC \frac{\alpha_3}{\alpha_2} + 1)x_1 + LC(\frac{\alpha_1}{\alpha_2} - \frac{1}{LC})x_2 < 0 \quad (24)$$

$$\lambda_2 = (LC \frac{\alpha_3}{\alpha_2} + 1)x_1 + LC(\frac{\alpha_1}{\alpha_2} - \frac{1}{R_L C})x_2 - (V_{ref} + \beta V_{in}) > 0 \quad (25)$$

The aforementioned conditions are shown in Fig. 9, for the two situations a)  $\frac{\alpha_1}{\alpha_2} > \frac{1}{R_L C}, \frac{\alpha_3}{\alpha_2} < \frac{-1}{LC}$  and b)  $\frac{\alpha_1}{\alpha_2} < \frac{1}{R_L C}, \frac{\alpha_3}{\alpha_2} < \frac{-1}{LC}$ .



In both figures, region 1 depicts  $\lambda_1 < 0$  and region 2 represents  $\lambda_2 > 0$ . The SM operation is only

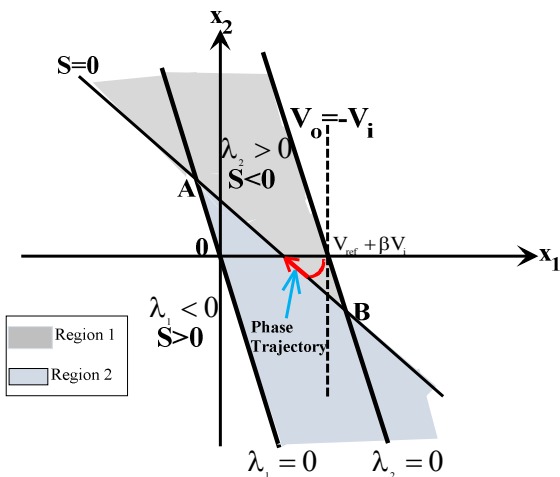


Fig. 9. Regions of SM existence in phase plane a)  $\frac{\alpha_1}{\alpha_2} > \frac{1}{R_L C}, \frac{\alpha_3}{\alpha_2} < \frac{-1}{LC}$  and b)  $\frac{\alpha_1}{\alpha_2} < \frac{1}{R_L C}, \frac{\alpha_3}{\alpha_2} < \frac{-1}{LC}$

valid on the portion of the sliding line  $S=0$ , that covers both regions 1 and 2. In this case the portion is within A and B, where A is intersection of  $S=0$  and  $\lambda_1=0$ , and B is the intersection of  $S=0$  and  $\lambda_2=0$ . Trajectory touches the sliding line  $S=0$

within AB, and slides through it. When trajectory goes beyond sliding line outside AB, it results an overshoot, when  $\frac{\alpha_1}{\alpha_2} > \frac{1}{R_L C}, \frac{\alpha_3}{\alpha_2} < \frac{-1}{LC}$ .

### 5 Incremental Conductance MPPT

Inc Cond MPPT controller algorithm with a fixed step size tracks MPP accurately. The flowchart of the controller is shown in Fig. 10. It tracks MPP

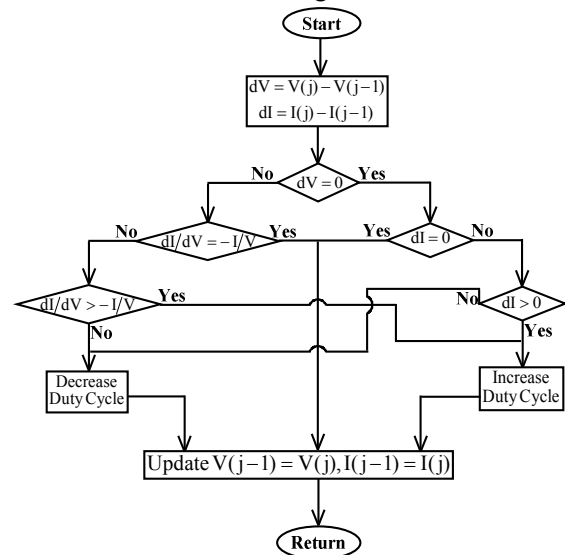


Fig. 10. Flow chart of Inc conductance MPPT controller

fastly, when compared to the other MPPT techniques [15].The controller is connected in an open loop. The controller measures the incremental changes in PV array current and voltage to predict the effect of voltage change. This method utilizes incremental conductance ( $dI/dV$ ) of a PV array to compute the sign of change in power with respect to voltage ( $dP/dV$ ).The Inc cond controller compares incremental conductance ( $\Delta I/\Delta V$ ) to array conductance ( $I/V$ ), and the difference of these two is zero then that voltage is MPP voltage, corresponding current is MPP current. Inc cond controller maintains the MPP voltage until the irradiation changes and the process is repeated. MPP is located at the knee of the I-V curve, where the resistance is equal to the negative of differential resistance[3].

$$\frac{V}{I} = -\frac{V}{I} \quad (26)$$

The slope of the PV curve at MPP is equal to zero.

$$\frac{dP}{dV} = 0 \quad (27)$$

After mathematical calculations (27), finally

$$I + V \frac{dI}{dV} = 0 \tag{28}$$

Based on (26) and (27) if any small error occurs then (28) becomes

$$I + V \frac{dI}{dV} = e \tag{29}$$

The error chosen on the basis of trial and error method and the error is 0.0024. According to the MPPT algorithm in the flowchart, duty cycle is calculated. Setting a new duty cycle in the system is repeated according to the sampling time.

### 6 Results And Discussion

An inc cond MPPT controller is a generic open loop controller; it is one of the widely used techniques to track MPP. This algorithm is developed with fixed step size. Here the outputs of inc cond and SMC controllers are presented and verified that, the SMC reached steady state condition very quickly and tracks excess power than inc cond controller. Implementation results of the inc cond controller and SMC in MATLAB/ SIMULINK is shown in Fig. 11 and Fig. 12. The electrical parameters of PV array are listed in Table 1 and tracking performances of the controllers are given in Table 2.

### 7 Conclusions

In this paper, modified SMC for boost converter is implemented with three basic steps which are (i) Hitting (ii) Existence (iii) Stability. The modified SMC tracks PV voltage swiftly and reaches steady state condition at 0.1s. The outputs of SMC is compared with a inc cond MPPT controller and observed that SMC will reach steady state faster. Phase trajectories at different conditions and SM existence conditions were plotted. Mathematical modeling of a PV cell is analyzed and the output of

Table 1  
Electrical Parameters of PV Array

Maximum power ( $P_{max}$ )	72W
Voltage at MPP ( $V_{MPP}$ )	18V
Current at MPP ( $I_{MPP}$ )	3.13A
Open circuit voltage ( $V_{oc}$ )	23V
Short circuit current ( $I_{sc}$ )	3.46A

PV array is connected to a DC DC boost converter for voltage regulation. State space analysis of a boost converter is derived and eventually a boost converter based SMC is developed. With this modi-

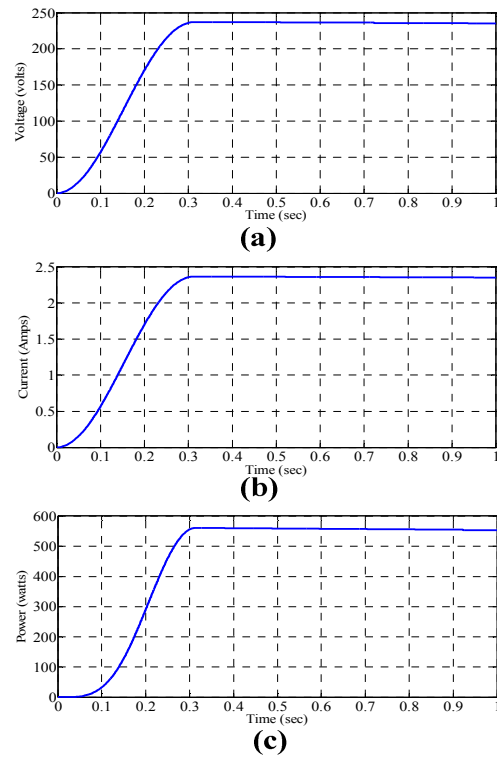


Fig. 10. Outputs of a Boost converter with conventional inc cond MPPT (a) Voltage, (b) Current, (c) Power.

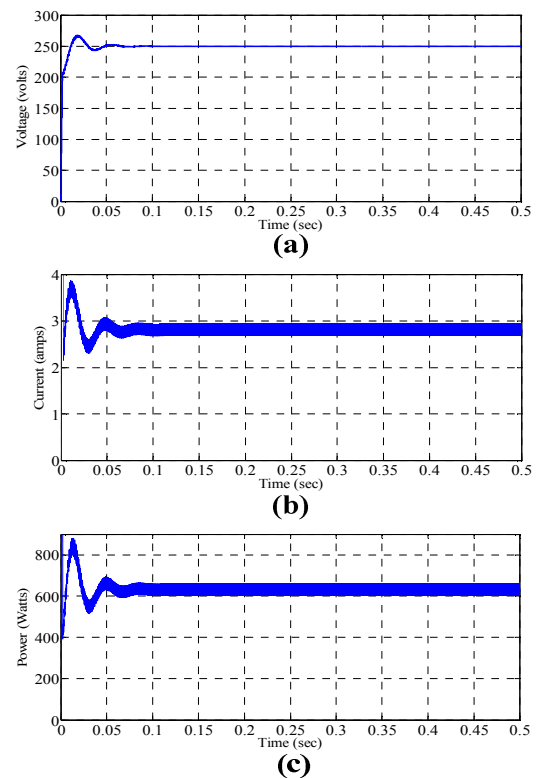


Fig. 11. Outputs of a Boost converter with modified SMC (a) Voltage (b) Current (c) Power.

Table 2  
Comparison of control Techniques

	SMC	Inc cond MPPT
Output Voltage	250V	235V
Output Current	2.5A	2.4A
Output Power	625W	563W

-fied SMC, the reference voltage level and steady state conditions occurred quickly and the results were compared with that of an MPPT controller.

#### References:

- [1] M.G.Villalva, J.R.Gazoli and E.R.Filho, *Comprehensive approach to modeling and simulation of photovoltaic arrays*, IEEE Trans. Power Electron., Vol. 24, No. 5, 2009, pp. 1198-1208.
- [2] R.J.Wai, W.H.Wang and C.Y.Lin, *High performance stand alone photovoltaic generation system*, IEEE Trans. Ind. Electron., Vol. 55, No. 1, 2008, pp. 240-250.
- [3] V.R.Kolluru, K.K.Mahapatra and B.Subudhi, *Development and implementation of control algorithms for a photovoltaic system*, IEEE conf. SCES, 2013, pp. 1-5.
- [4] Y.Hsieh, J.Chen, T.Liang and L.Yang, *Novel high step up DC DC converter with coupled inductor and switched capacitor techniques for a sustainable energy system*, IEEE Trans. Power Electronics, Vol. 26, No. 12, 2011, pp. 3481-3490.
- [5] S.C.Tan, Y.Lai and C.Tse, *Sliding Mode Control of Switching Power Converters Techniques and implementation*, 1<sup>st</sup> ed. Boca Raton, FL: CRC, 2012.
- [6] S.C.Tan, Y.Lai and C.Tse, *General desing issues of sliding mode controllers in dc-dc converters*, IEEE Trans. Ind. Electron., Vol. 55, No. 3, 2008, pp. 1160-1174.
- [7] S.C.Tan, Y.M.Lai, C.K.Tse, L.M.Salamero and C.K.Wu, *A fast response sliding mode controller for boost type converters with wide range of operating conditions*, IEEE Trans. Ind. Electron., Vol. 54, No. 6, 2007, pp. 3276-3286.
- [8] V.R.Kolluru, K.K.Mahapatra and B.Subudhi, *Design and implementation of modified sliding mode controller for a photovoltaic system*, IEEE conf. ICAEE'14, 2014, pp. 1-6.
- [9] Y.Levron and D.Shmilovitz, *Maximum power point tracking employing sliding mode control*, IEEE Trans. Circuits Syst. I, Reg. Papers, Vol. 60, No. 3, 2013, pp. 724-732.
- [10] H.Li and X.Ye, *Sliding mode PID control of dc-dc converter*, IEEE Int. Conf., 2010, pp.730-734.
- [11] H.Guldemir, *Sliding mode control of dc-dc boost converter*, Journal of Appl. Sci., Vol. 5, No. 3, 2005, pp. 588-592.
- [12] Y.P.Jiao and F.L.Luo, *An improved sliding mode controller for boost cinverter in solar energy system*, IEEE Int. Conf. ICIEA, 2009, pp. 805-810.
- [13] J.F.Tsai and Y.P.Chen *Sliding mode control and stability analysis of buck dc-dc converter*, Int. Journal of Elect., Vol. 94, No. 3, pp. 209-222.
- [14] F.Inthamoussou, H.D.Battista and M.Cendoya, *Low cost sliding mode power controller of a stand alone photovoltaic module*, IEEE Int. Conf. ICIT, 2010, pp. 1175-1180.
- [15] B.Subudhi, R.Pradhan, *A comparative study on maximum power point tracking techniques for photovoltaic power systems*, IEEE Trans. Sustain. Energy, Vol. 4, No. 1, 2013, pp. 89-98.
- [16] R.Gules, J.D.P.Pacheco, H.L.Hey and J.Imhoff, *A maximum power point tracking system with parallel connection for PV stand alone applications*, IEEE Trans. Ind. Electron. Vol. 55, No. 7, 2008, pp. 2674-2683.
- [17] S.B.Kjaer, *Evaluation of the hill climbing and the incremental conductance maximum power point trackers for photovoltaic power systems*, IEEE Trans. Energy Conversion, Vol. 27, No. 4, 2012, pp.922-929.
- [18] F. Attivissimo, A.D.Nisio, M.Savino and M. Spadavecchia, *Uncertainty analysis in photovoltaic cell parameter estimation*, IEEE Trans. Instr. and Measure., Vol. 61, No. 5, 2012, pp. 1334-1342.
- [19] Q.Mei, M.Shan, L.Liu and J.M.Guerrero, *A novel improved variable step size incremental resistance MPPT method for PV systems*, IEEE Trans. Ind. Electron., Vol. 58, No. 6, 2011, pp. 2427-2434.
- [20] L.Zhang, W.G.Hurley and W.H.Wolfle, *A new approach to achieve maximum powr point tracking for PV system with a variable inductor*, IEEE Trans. Power Electronics, Vol. 26, No. 4, 2011, pp. 1031-1037.